

Evidence of A Simple Dark Sector from XENON1T Anomaly

Cheng-Wei Chiang^{1,*} and Bo-Qiang Lu^{1,†}

¹*Department of Physics, National Taiwan University, Taipei, Taiwan 10617, Republic of China*

We propose that the nearly massless dark photons produced from the annihilation of keV dark fermions in the Galaxy can induce the excess of electron recoil events recently observed in the XENON1T experiment. The minimal model for this is the extension of a $U(1)_X$ gauge symmetry, under which the dark photon couples to both dark and visible matter currents. We find that the best-fit parameters of the dark sector are compatible with the most stringent constraints from stellar cooling. The dark fermion relic density in both freeze-in and freeze-out scenarios has been calculated and found to be able to account for the observed dark matter abundance.

Introduction — One of the outstanding puzzles in particle physics is the nature of dark matter (DM), whose existence has been confirmed from various cosmological and astrophysical observations [1]. An attractive hypothesis, the weakly interacting massive particles (WIMPs) [2] having mass at around the electroweak scale and coupling strength similar to the weak coupling, have suffered stringent constraints from both direct [3] and indirect [4] DM detection experiments. As alternatives to the WIMP DM, sub-GeV or (super-)light DM candidates, such as axion and dark photon, have drawn more attention in recent years.

The result of searches for new physics using low-energy electronic recoil data recently published by XENON Collaboration shows an excess of events over the known backgrounds in the recoil energy range 1–7 keV, peaked around 2.4 keV, with a local statistical significance of $3\text{--}4\sigma$ [5]. A series of theoretical works have been inspired to explain the origin of the excess (see Ref. [6] for a summary). As noted by the XENON Collaboration, the absorption of axions emitted by the Sun can fit the data quite well. However, the favored parameter space is in severe tension with stellar cooling constraints [5]. If axion-like particles (ALPs) are assumed to be the sole DM that couple predominantly to electrons (the so-called photophobic models), the XENON1T anomaly can be explained without being excluded by the constraints [6]. The Dine-Fischler-Srednicki-Zhitnitsky [7] type of ALPs are excluded by the stellar cooling since they strongly couple to both electrons and photons. XENON1T experiment is in general insensitive to the Kim-Shifman-Vainshtein-Zakharov [8] type of ALPs which couple to electron at the loop level [5]. The absorption of massive dark photon DM also suffer strong constraints from stellar cooling observations [9]. DM accelerated by the Sun or cosmic rays to higher velocities can scatter with the electrons and result in a keV-scale energy deposition [10]. For such scenarios, a dramatic conflict with lower-threshold direct-detection searches from XENON1T (S2-only) and SENSEI arises because of the steeply rising DM-electron scattering form factor at low-momentum transfers [6]. Furthermore, Super-K experiment and stellar cooling observations also impose strin-

gent constraints on this scenario.

In this Letter, we propose the dark fermion annihilation to nearly massless (compared to the keV scale) dark photons in the Galaxy as the origin for the XENON1T anomaly. Comparing with the explanations mentioned above, our scenario is simpler and more natural. As shown below, our scenario can survive the most stringent constraints from stellar cooling observations and the XENON1T data can be accommodated even when the dark fermions constitute only a small fraction of the DM.

Dark Sector — Consider a simple extension of the Standard Model (SM) with a dark $U(1)_X$ gauge symmetry, with the gauge field denoted by \tilde{X}_μ , and a Dirac dark fermion χ carrying $U(1)_X$ charge $q_X = 1$. SM particles are all neutral under the $U(1)_X$ gauge symmetry. The relevant Lagrangian describing the dark sector, the photon field, and the mixing between the visible and dark photons reads

$$\mathcal{L}_0 = -\frac{1}{4}X_{\mu\nu}X^{\mu\nu} - \frac{1}{4}F_{\mu\nu}F^{\mu\nu} - \frac{\varepsilon}{2}X_{\mu\nu}F^{\mu\nu} + \bar{\chi}(i\cancel{D} - m_\chi)\chi, \quad (1)$$

where $X_{\mu\nu} = \partial_\mu\tilde{X}_\nu - \partial_\nu\tilde{X}_\mu$ and $F_{\mu\nu} = \partial_\mu\tilde{A}_\nu - \partial_\nu\tilde{A}_\mu$, and the covariant derivative $D_\mu = \partial_\mu - ie_X q_X \tilde{X}_\mu$, with e_X denoting the dark gauge coupling. The parameter $\varepsilon \ll 1$ represents the kinetic mixing between the dark gauge boson \tilde{X}_μ and the $U(1)_{\text{em}}$ gauge boson \tilde{A}_μ .

The kinetic terms of gauge boson in the Eq. (1) can be diagonalized by rotating the gauge fields as

$$\begin{pmatrix} \tilde{X}_\mu \\ \tilde{A}_\mu \end{pmatrix} = \begin{pmatrix} 1 & 0 \\ -\varepsilon & 1 \end{pmatrix} \begin{pmatrix} \cos\theta & -\sin\theta \\ \sin\theta & \cos\theta \end{pmatrix} \begin{pmatrix} X_\mu \\ A_\mu \end{pmatrix}, \quad (2)$$

where we now identify A_μ as the visible photon and X_μ as the dark photon. The rotation angle θ would be locked at zero if the dark photon becomes massive from gauge symmetry breaking [11]. In this case, the nearly massless dark photon X_μ couples to both visible and dark currents while the ordinary photon A_μ couples exclusively to the visible current:

$$\mathcal{L} = eJ^\mu A_\mu + (e_X J_X^\mu - \varepsilon e J^\mu) X_\mu, \quad (3)$$

where e is the electric charge, J^μ is the visible current, and $J_X^\mu = \bar{\chi}\gamma^\mu\chi$ is the dark current.

Our interpretation for the XENON1T excess is the following. The dark fermions χ pair annihilate into the dark photon pairs via the t and u -channel exchanges, and the dark photons are absorbed by the detector material and lead to the electron emissions because of the dark photoelectric effect. Since the dark fermions are nonrelativistic, each of the dark photons thus produced has energy $E_{\gamma'} = m_\chi$. Furthermore, the dark fermion annihilation into other SM particles is kinematical forbidden when $m_\chi < m_e = 511$ keV. Note that the mean free path of keV visible photons in the atmosphere is $l_\gamma = 1/(\rho_{\text{gas}}\sigma_\gamma^{\text{gas}}(\text{keV})) \sim 1$ cm due to strong absorption. Hence, such photons produced in the space would not be able to reach the detector on Earth. In contrast, the mean free path of keV dark photon in the atmosphere can be estimated to be $l_{\gamma'} = l_\gamma/\varepsilon^2$. Provided that the mixing parameter $\varepsilon \sim 10^{-10}$, the mean free path of keV dark photon is then $\sim 10^{20}$ cm, much larger than the Earth radius $r_e = 6.37 \times 10^8$ cm. Thus, the atmosphere is transparent to the keV dark photons.

XENON1T Excess — The differential dark photon flux from dark fermion annihilation is given by [4]

$$\frac{d\Phi_{\gamma'}}{dE_{\gamma'}} = \frac{\langle\sigma v\rangle_{\gamma'\gamma'}}{2m_\chi^2} \frac{dN_{\gamma'}}{dE_{\gamma'}} J_\chi, \quad (4)$$

where the dark fermion J -factor is $J_\chi = \frac{1}{4\pi} \int d\Omega \int ds p_\chi^2$. Suppose the dark fermions constitute a fraction of the observed DM, *i.e.*, the dark fermion density and the DM mass density are related by $\rho_\chi = f_\chi \rho_{\text{DM}}$ with $f_\chi \leq 1$. Here we assume the NFW profile [12] for the Galactic DM halo profile

$$\rho_{\text{DM}}(r) = \frac{\rho_s}{(r/r_s)(1+r/r_s)^2}, \quad (5)$$

where $r_s = 20$ kpc and $\rho_s = 0.26$ GeV cm $^{-3}$, corresponding to a local DM mass density 0.3 GeV cm $^{-3}$. The dark fermion J -factor is then determined by $J_\chi = f_\chi^2 J_{\text{DM}} \simeq f_\chi^2 \times 10^{22}$ GeV 2 cm $^{-5}$ [4]. The dark photon energy spectrum is

$$\frac{dN_{\gamma'}}{dE_{\gamma'}} = 2\delta(E_{\gamma'} - m_\chi). \quad (6)$$

Since the annihilation can proceed through s -wave processes, the thermally averaged cross section $\langle\sigma v\rangle_{\gamma'\gamma'}$ at the leading order is given by

$$\langle\sigma v\rangle_{\gamma'\gamma'} \simeq \frac{\pi\alpha_X^2}{2m_\chi^2} + \mathcal{O}(v^2), \quad (7)$$

with $\alpha_X \equiv e_X^2/(4\pi)$.

The event rate due to the absorption of dark photons produced from dark fermion annihilation in the detector is given by [13]

$$\frac{dR(E)}{d\Delta E} = \int dE_{\gamma'} \sigma_{\gamma'}(E_{\gamma'}) \frac{d\Phi_{\gamma'}}{dE_{\gamma'}} \epsilon(E) MT \frac{1}{\sqrt{2\pi}\sigma} e^{-\frac{(E-E_{\gamma'})^2}{2\sigma^2}} = \frac{\sigma_{\gamma'}(m_\chi) \langle\sigma v\rangle_{\gamma'\gamma'}}{\sqrt{2\pi}\sigma} \frac{J_\chi \epsilon(E) MT e^{-\frac{(E-m_\chi)^2}{2\sigma^2}}}{m_\chi^2}, \quad (8)$$

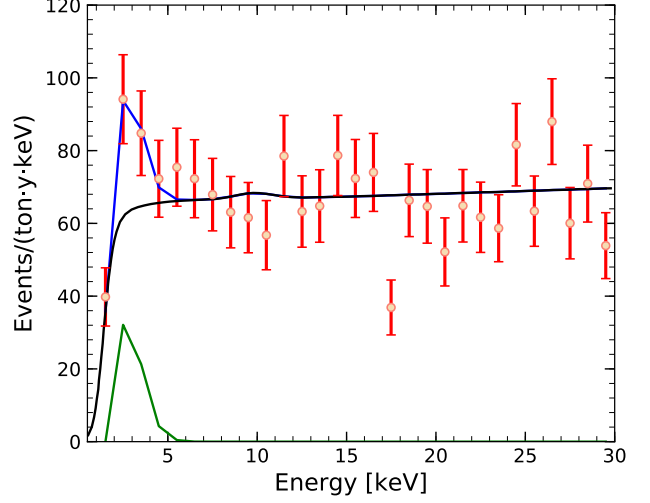


FIG. 1. The energy spectrum of recoiled electrons for the benchmark of $m_\chi = 3.17$ keV and $\alpha' = 1.46 \times 10^{-21}$, represented by the blue curve. The data and background (black curve) are extracted from Ref. [5]. The green curve represents the contribution from the absorption of dark photons.

where $\sigma_{\gamma'} = \varepsilon^2 \sigma_\gamma$ is the dark photoelectric cross section of the detector material for photons with energy $E_{\gamma'}$, with the photoelectric cross section σ_γ given in Ref. [14]; $\epsilon(E)$ is the total efficiency for the XENON1T experiment; $MT = (1042 \text{ kg}) \times (226.9 \text{ days})$ is the exposure; and σ is the experimental energy resolution [15]. A fit to the experimental energy resolution data distribution gives $\sigma/E = 0.341/\sqrt{E}$. With Eq. (4) to Eq. (8), the event rate is then estimated to be

$$\frac{dR}{d\Delta E} = 1.737 \times 10^{40} (f_\chi \alpha')^2 \epsilon(E) \left(\frac{\text{keV}}{m_\chi} \right)^4 \left(\frac{\sigma_\gamma(m_\chi)}{\text{barns}} \right) \times \frac{1}{\sqrt{2\pi}\sigma} e^{-\frac{(E-m_\chi)^2}{2\sigma^2}}, \quad (9)$$

where $\alpha' \equiv \varepsilon \alpha_X = \varepsilon e_X^2/(4\pi)$. If we assume that the DM is entirely comprised of the dark fermions, *i.e.*, $f_\chi = 1$, $\alpha' \sim 10^{-21}$ is sufficient to generate ~ 10 photoelectric events in the XENON1T detector, using the xenon photoelectric cross section $\sigma_\gamma(3 \text{ keV}) \sim 10^5$ barns/atom. Fig. 1 shows the predicted energy spectrum. The signal events represented by the green curve are calculated using the benchmark parameters $m_\chi = 3.17$ keV and $\alpha' = 1.46 \times 10^{-21}$. The data points and background events (black curve) are taken from Ref. [5]. The blue curve represents the total events in our model.

In Fig. 2, we depict the parameter region favored by the XENON1T data at 1σ (dark green curves) and 2σ (light green curves) confidence level (C.L.). The solid curves are drawn for the scenario when all the DM are explained by the dark fermion, whereas the dashed curves are for the scenario when the dark fermion constitutes 1% of the DM relic density. To do this, we calculate

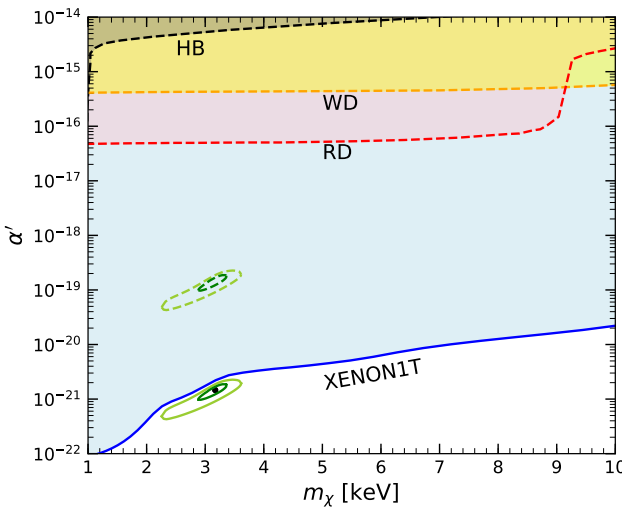


FIG. 2. The solid (dashed) green contours represent the parameter region favored by the XENON1T data for $f_\chi = 1$ (10^{-2}) at the 1σ (darker) and 2σ (lighter) levels. For $f_\chi = 1$, the 95% C.L. upper limits on α' as derived from the XENON1T data is represented by the blue curve. The constraints from red giants (RD), white dwarves (WD), and horizontal branch (HB) stars are taken from Ref. [16].

the signal and background from Ref. [5] in 29 equidistant bins between 1 keV and 30 keV. The goodness of the fit to data is estimated using a χ^2 test. We find that the best-fit parameters are $m_\chi = 3.17 \pm 0.21$ keV and $\alpha' = (1.46 \pm 0.44) \times 10^{-21}$, marked by the black dot in the figure, with $\chi^2_{\text{min}}/\text{d.o.f} = 35.90/27$ (corresponding to a p -value of 11.75%). A purely background fit to the data gives $\chi^2_{\text{bkg}} = 46.35/29$ (p -value = 2.17%). We also derive the 95% C.L. upper limits on the coupling α' for a given value of m_χ by increasing the minimum χ^2 by $\Delta\chi^2 = 5.99$. Such a limit is given by the blue curve, and the light-blue region is excluded at 95% C.L.

For the dark fermion mass in the range $m_\chi \lesssim 10$ keV, the most relevant and stringent constraints come from astrophysical observations of stellar evolution. The stellar energy loss due to the emission of dark fermions and dark photons can reduce the helium flash in red giants and accelerate the helium-burning stage and the cooling of white dwarves. We take the constraints from red giants (RD), white dwarves (WD), as well as horizontal branch (HB) stars from Ref. [16], and convert them to the corresponding limits on α' as a function of m_χ . The colored regions in Fig. 2 are excluded by the constraints at 95% C.L. We find that the regions (with $f_\chi = 1$) inferred from the XENON1T experiment is far below the constraints from stellar cooling. In fact, the allowed parameter space is so large that even if the dark fermion constitutes only a small fraction ($f_\chi \sim 10^{-3} - 10^{-2}$) of DM, the dark fermion annihilation can still possibly account for the XENON1T excess (as shown by the example of dashed green contours for $f_\chi = 10^{-2}$). Hence, our model can

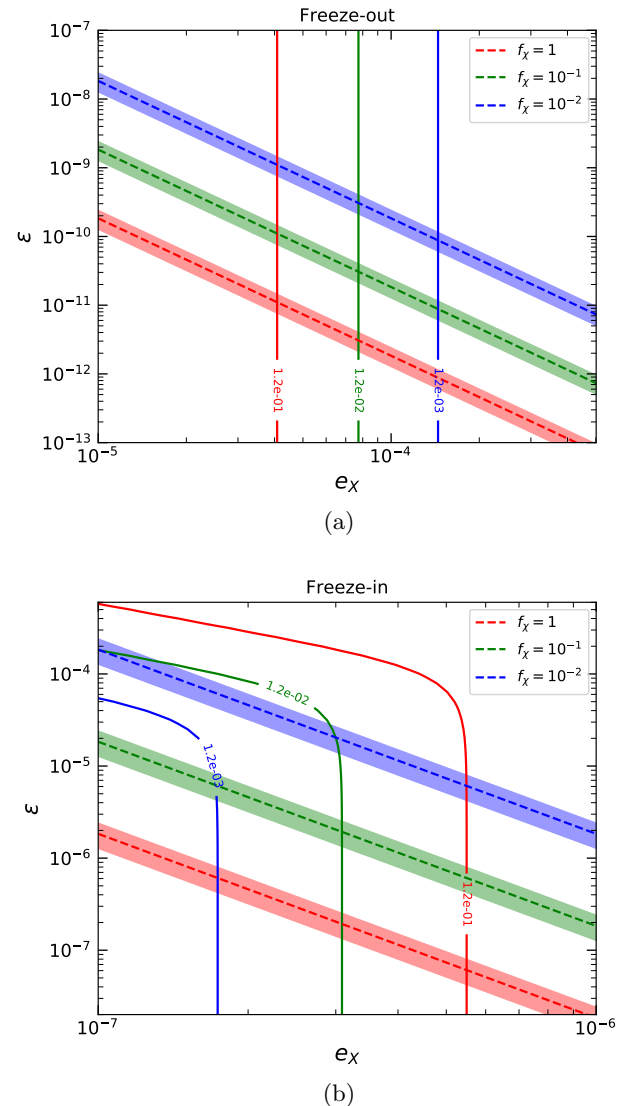


FIG. 3. The solid curves correspond to the dark fermion relic density $\Omega_\chi h^2 = 0.12$ (red), 0.012 (green), and 0.0012 (blue), and the dashed curves correspond to the best-fit value of α' in the corresponding case in the $ex - \epsilon$ plane. The colored bands represent the 1σ uncertainty in α' . Plot (a) and plot (b) are for the freeze-out and freeze-in scenarios, respectively. The dark fermion mass is fixed at 3.17 keV in both plots, and the relic density is calculated with the help of MicrOMEGAs_5.0.4 [20].

readily explain the XENON1T excess without causing any tension with astrophysical observations. We note in passing that owing to the absence of photon pair annihilation in our model at tree level, the constraints arising from the observational X-ray data [17] can be avoided. In the limit of massless dark photon considered here, constraints for the massive dark photon from cosmological [18] and astrophysical [19] observations do not apply.

Relic Density— It is natural to ask how the light dark fermion becomes part of the DM and whether there exists parameter space that satisfies both the

XENON1T experiment and the DM relic density [1]. From now on, we fix the dark fermion mass at the preferred value $m_\chi = 3.17$ keV determined above. If the dark fermions decouples from the thermal equilibrium in the early Universe when they are still relativistic, their current relic abundance is determined by $\Omega_\chi h^2 = (4.67 \times 10^2 / g_*(T_f))(m_\chi / 3.17 \text{ keV})$, where $g_*(T_f)$ is the number of relativistic degrees of freedom in the dark sector at the decoupling temperature T_f . A large value of $g_* \simeq 4 \times 10^3$ is required to reproduce the DM relic density, which is fairly impossible in the current model. In the freeze-out scenario, the dark fermions are initially in thermal equilibrium with other particles and decouple from the thermal bath as the temperature drops. The solid curves in Fig. 3(a) are for different relic densities of dark fermion produced via the freeze-out mechanism. Note that they have no dependence on the mixing parameter ε , as a result of the fact that the dark fermion annihilation to SM charged fermions is kinematically forbidden. The dashed curves represent the best-fit value of α' in the e_X - ε plane, with various choices of f_χ and the colored bands representing the 1σ uncertainty. The intersection between the solid and dashed curves of the same color determines those parameters that satisfy the XENON1T excess while producing the correct fractional relic density of DM.

If the dark fermions do not reach thermal equilibrium with other particles in the early Universe, its relic abundance can be obtained via the freeze-in mechanism [21], as shown in Fig. 3(b). In addition to the dark photon pair annihilation, the SM charged fermion annihilation to the dark fermions in the freeze-in scenario is also allowed and its cross section is proportional to $\varepsilon^2 e_X^4$. For sufficiently small values of e_X , the latter plays some role in determining the dark fermion relic density. As e_X increases to a certain value, however, the relic density becomes insensitive to ε because the former dominates the dark fermion production. As shown in the plot, the fractional DM relic density of the dark fermion via freeze-in should be in the range of 0.1–1, outside which no intersection between the solid and dashed curves of the same color can be found. Both plots show that the dark photon pair channel dominates the determination of dark fermion relic density in the early Universe and that plenty of parameter space is available for explaining the XENON1T excess.

Summary— We have proposed that the anomalous excess in the electron recoil events in XENON1T experiment can be owing to the effect of (nearly) massless dark photons produced from the annihilation of keV dark fermion in the Galaxy, and the dark fermion can constitute part of or entirely the dark matter relic density, depending on the parameters and scenario. In particular, the required parameters for explaining the XENON1T excess and the DM relic density in the minimum model presented here are fully compatible with the constraints from stellar cooling. Future multi-ton underground ex-

periments shall be able to shed further light on the XENON1T anomaly and provide more opportunities to observe the dark sector.

Acknowledgments— This work was supported in part by the Ministry of Science and Technology (MOST) of Taiwan under Grant Nos. MOST-108-2112-M-002-005-MY3 and MOST-108-2811-M-002-548.

* chengwei@phys.ntu.edu.tw

† bqlu@phys.ntu.edu.tw

- [1] Planck Collaboration, *Astron. Astrophys.* **594**, A13 (2016).
- [2] B. W. Lee and S. Weinberg, *Phys. Rev. Lett.* **39**, 165 (1977).
- [3] XENON Collaboration, *Phys. Rev. Lett.* **121**, 111302 (2018).
- [4] Fermi LAT Collaboration, *Phys. Rev. Lett.* **115**, 231301 (2015).
- [5] XENON Collaboration, arXiv:2006.09721.
- [6] I. M. Bloch, A. Caputo, R. Essig, D. Redigolo, M. Sholapurkar, and T. Volansky, arXiv:2006.14521.
- [7] M. Dine, W. Fischler, and M. Srednicki, *Phys. Lett. B* **104**, 199 (1981); A. Zhitnitskii, *Sov. J. Nucl. Phys.* **31**, 260 (1980).
- [8] J. E. Kim, *Phys. Rev. Lett.* **43**, 103 (1979); M. Shifman, A. Vainshtein, and V. Zakharov, *Nucl. Phys. B* **166**, 493 (1980).
- [9] G. Alonso-Alvarez, F. Ertas, J. Jaeckel, F. Kahlhoefer and L. J. Thormaehlen, arXiv:2006.11243; H. An, M. Pospelov, J. Pradler, and A. Ritz, arXiv:2006.13929.
- [10] H. An, M. Pospelov, J. Pradler, and A. Ritz, *Phys. Rev. Lett.* **120**, 141801 (2018); T. Bringmann and M. Pospelov, *Phys. Rev. Lett.* **122**, 171801 (2019); B. Fornal, P. Sandick, J. Shu, M. Su, and Y. Zhao, arXiv:2006.11264; Q.-H. Cao, R. Ding, and Q.-F. Xiang, arXiv:2006.12767.
- [11] M. Fabbrichesi, E. Gabrielli and G. Lanfranchi, arXiv:2005.01515.
- [12] J. F. Navarro, C. S. Frenk, and S. D. M. White, *Astrophys. J.* **490**, 493 (1997).
- [13] EDELWEISS Collaboration, *J. Cosmol. Astropart. Phys.* **11**, 067 (2013).
- [14] W. M. J. Veigle, *Atomic Data Table* **5**, 51 (1973); M. J. Berger, *et al.*, XCOM: Photon cross sections database, <http://www.nist.gov/pml/data/xcom/index.cfm>.
- [15] XENON Collaboration, *Nature* **568**, 532535 (2019).
- [16] H. Vogel and J. Redondo, *J. Cosmol. Astropart. Phys.* **02**, 029 (2014).
- [17] S. Riemer-Sørensen, *Astron. Astrophys.* **594**, A71 (2016).
- [18] S. D. McDermott and S. J. Witte, *Phys. Rev. D* **101**, 063030 (2020).
- [19] H. An, M. Pospelov, and J. Pradler, *Phys. Lett. B* **725**, 190195 (2013).
- [20] D. Barducci *et al.*, *Comput. Phys. Commun.* **590**, 327 (2018).
- [21] L. J. Hall, K. Jedamzik, J. March-Russell, and S. M. West, *J. High Energy Phys.* **03**, 080 (2010).